

Fully Automated Assessment of Left Ventricular Volumes and Mass from Cardiac Magnetic Resonance Images

M. Marino, F. Veronesi, C. Corsi

Abstract – Quantification of left ventricular (LV) size and function from cardiac magnetic resonance (CMR) images requires manual tracing of LV borders on multiple 2D slices, which is subjective, tedious and time-consuming experience. This paper presents a fully automated method for endocardial and epicardial boundaries detection for the assessment of LV volumes, ejection fraction (EF) and mass from CMR images. The segmentation procedure is based on a combined level set approach initialized by an automatically detected point inside the LV cavity. To validate the proposed technique, myocardial boundaries were manually traced on end-diastolic (ED) and end-systolic (ES) frames by an experienced cardiologist. Bland-Altman analysis and linear regression were used to validate LV volumes, EF and mass and similarity metrics were applied to assess the agreement between manually and automatically detected contours. We found minimal biases and narrow limits of agreement for LV volumes, EF and mass; Dice coefficient, Jaccard index and Hausdorff distance evaluated for 2D ED and ES endocardial and epicardial boundaries showed adequate overlapping. The proposed technique allows fast and accurate assessment of LV volumes, EF and mass as a basis for accurate quantification of LV size and function, and myocardial scar from CMR images.

I. INTRODUCTION

Cardiac Magnetic Resonance (CMR) provides a high resolution, radiation free, dynamic imaging of the heart. These features allowed this methodology to become the standard reference technique for accurate and reproducible evaluation of LV volumes and function [1]. Although automated left ventricular (LV) endocardial boundary detection is available in commercial software for analysis of CMR images, it is usually based on algorithm parameters that are sensitive to image quality and frequently depend on the specific imaging protocol [2]. Since optimization of these parameters is not possible, the computation of LV volumes and EF in clinical practice relies on frame-by-frame manual tracing of endocardial contours on multiple 2D short-axis planes. This procedure is subjective, depending from cardiologist experience, tedious and time-consuming, due to

the huge amount of acquired images. Consequently, clinical assessment of LV function is often limited to the quantitative analysis of end diastolic (ED) and end systolic (ES) frames, but this approach does not consider important dynamic information of the heart. Availability of a reliable technique for automated detection of LV borders could thus improve the accuracy of CMR quantification of LV volumes and mass and allow the assessment of diastolic and systolic function. Accordingly, the purpose of this study was to develop a fast and automated method for the dynamic detection of LV endocardial and epicardial boundaries from short-axis CMR images. The main steps of this method consisted in: 1) fully automated identification of the LV cavity based on the detection of moving and circular structures in the images [3][4]; 2) endocardium segmentation based on region-based probabilistic level set model [5][6]; 3) epicardium segmentation based on an edge-based level set model [7].

II. METHODS

A. CMR imaging

CMR data were obtained in 10 patients using a 1.5T Inera Achieva scanner (Philips Medical Systems, Best, the Netherlands) at the Cardiac Imaging Research of the University of Chicago, USA. Cine-loops were acquired during 10 to 15 second breatholds in 8 to 14 short axis slices from the atrio-ventricular ring to the apex using a steady-state free precession dynamic gradient-echo mode. The imaging parameters were as follows: echo time = 1 ms, repetition time = 3 ms, flip angle = 60°, slice thickness = 8 mm with no gaps, scan matrix size = 256 x 256 and pixel spacing = 1.40 mm². Temporal resolution was 30 frames for cardiac cycle.

B. Image Analysis

LV slices were selected for analysis beginning with the highest basal slice where the LV outflow tract was not visible, and ending with the lowest apical slice where the LV cavity was visualized. LV endocardial and epicardial contours at the ED and ES were manually traced with the papillary muscles in the LV cavity, by an experienced investigator. This resulted in LV cross-sectional area for each slice over time. Global LV volumes were computed throughout the cardiac cycle using a disk-area summation method, from which end-diastolic and end-systolic volumes (EDV and ESV, respectively) were obtained as the

M. Marino is with University of Bologna, Cesena Campus, Via Venezia 52, Cesena, 47521, ITALY; e-mail: marco.marino7@studio.unibo.it.

F. Veronesi is with University of Bologna, Department of Electric, Electronic and Information Engineering "Guglielmo Marconi" - DEI, Bologna, ITALY.

C. Corsi is with University of Bologna, Department of Electric, Electronic and Information Engineering "Guglielmo Marconi" - DEI, Bologna, ITALY.

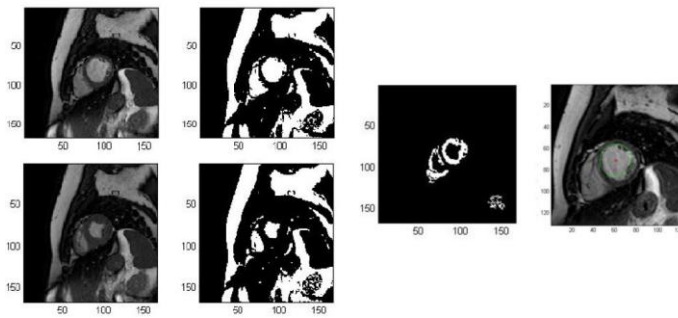


Figure 1. LV cavity identification: mid ED and 15th frame images (first column on the left) were converted into binary images (second column); the “difference” image in the third column shows the moving structures corresponding to the ventricles; the Hough transform is applied to detect the circular shape corresponding to the LV chamber.

maximum and the minimum volumes and EF was calculated as $(EDV-ESV)/EDV \cdot 100$. LV mass was computed at ED as $1.05 \cdot (V_{\text{epi}} - EDV)$, where V_{epi} is the volume included in the epicardium.

CMR datasets were analyzed using custom software for automated LV endocardial and epicardial contours detection. The segmentation process required an initial condition that was automatically defined. LV cavity was identified by assuming the heart is the only moving structure in the CMR images; therefore we looked for the differences in ventricle morphology between ED and the fifteenth frames in the cardiac cycle, on a mid slice (Fig. 1). We roughly detected the left and right ventricles position and considering the LV shape is almost circular on short-axis images, the application of the Hough Transform for circular shape detection allowed us to select the LV [3][4]. The same process was then repeated for all slices, from base to apex. Images were then cropped around the detected areas to increase segmentation method robustness and reduce computational processing time. The center of the detected area was used to define the initial condition for the segmentation step on each acquired plan.

Endocardial boundaries were automatically detected applying a region-based level set segmentation procedure based on statistical model exploiting the information related to the image noise distribution [5][6]. This method drives the curve evolution to the slice partitioning into maximally homogeneous regions, which have different local noise patterns. Since the presence of papillary muscles and trabeculae did not allow an adequate delineation of the endocardial borders, the endocardial contour was corrected by applying an additional evolution only in a mask region, defined to automatically include papillary muscles and trabeculae inside the LV cavity. The mask was created considering the difference between the previously detected curve and a curve obtained by processing a filtered version of the original image applying the Perona-Malik anisotropic filter [7] to homogenize the gray levels intensity inside the LV chamber.

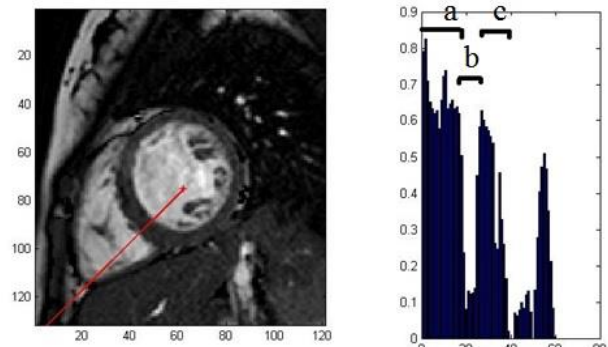


Figure 2. Evaluation of myocardial thickness: wall thickness was roughly computed in each slice starting from the radius marked from the previous endocardial initial point towards the right ventricle. The histogram along this direction allowed the detection of the LV cavity (a), of the RV cavity (c) and of the myocardial tissue (b).

Epicardial boundaries were obtained applying an edge-based level set model, based on curvature, ballooning and advection terms [8] and using the previously obtained mask as a weight matrix for the edge indicator. Initial condition for epicardial segmentation was set using the previously computed endocardium contour. Wall thickness was roughly evaluated considering the gray level histogram along specific direction automatically detected [9] and the endocardial curve was expanded considering this measurement (Fig. 2).

This segmentation procedure was applied for each slice at the ED frame. To extend the contour delineation throughout the cardiac cycle, we hypothesized the LV does not significantly move between subsequent frames. This assumption allowed to set, as initial condition for the following frames, the detected contours at previous frame. Contour refinement was obtained by simply applying the Malladi-Sethian model to adequately detect the LV endocardial and epicardial boundaries in the following frames. Matlab R2013a (The MathWorks Inc.) environment was used for software implementation.

C. Statistical Analysis and similarity indices

Statistical analysis was performed using Matlab software. Comparisons between automated and manual measurement of EDV, ESV, EF and mass included linear regression and Bland-Altman analyses. In addition, Hausdorff distance and similarity indices as Dice coefficient and Jaccard index were computed.

III. RESULTS

Standard time required for automated segmentation for all slices throughout the entire cardiac cycle was almost 6 minutes on a standard PC (Intel Core i5-2410M CPU @ 2.30 GHz, RAM 4 GB) for each patient. LV cavity was successfully identify in more than 97.5% of the analyzed images. LV chamber was not found in a few ES apical slices,

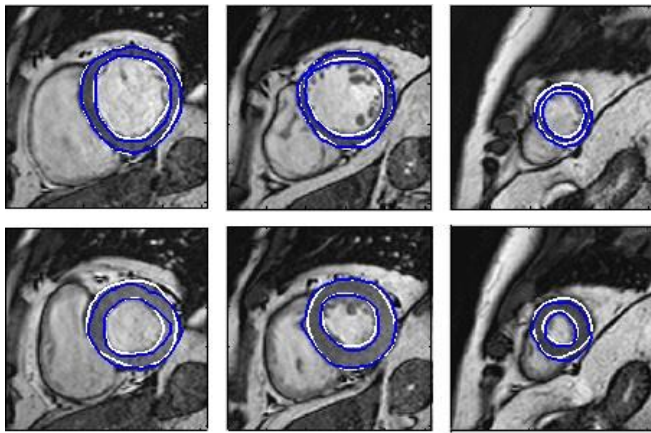


Figure 3. Example of the detected endocardial and epicardial contours in the ED (top) and ES (bottom) frames for LV basal, medial and apical slice (from the left to the right) obtained applying the automatic technique (blue) and the manually traced ones (white).

TABLE I. RESULTS OF THE BLAND-ALTMAN ANALYSIS

Parameters	Bias	Bias as error%/Mean	95% Limits of agreement	Mean
EDV	-7.48 ml	4.11 %	-21.97 ÷ 6.99 ml	181.56 ml
ESV	-3.03 ml	3.35 %	-22.73 ÷ 16.67 ml	90.37 ml
EF	0.18 %	0.35 %	-10.30 ÷ 10.66 %	50.22 %
Mass	-8.39 g	7.41 %	-23.88 ÷ 7.08 g	113.09 g

due to the smaller dimension and irregular shape of the cavity.

Fig. 3 shows an example of the LV endocardial and epicardial borders detected at ED and ES phase at different levels: basal, medial and apical slice. The automatically detected contours were superimposed to the manual traced contours to visually appreciate the overlapping agreement.

Linear regression analysis (Fig. 4-5) between the automated technique and the manual reference showed very good correlation coefficients and regression slopes for EDV ($y = 1.02x + 2.24$, $r^2 = 0.99$) and ESV ($y = 0.93x + 10.26$, $r^2 = 0.98$). High correlation and regression slope was also obtained for EF ($y = 0.89x + 5.5$, $r^2 = 0.92$) and mass ($y = 1.05x + 0.33$, $r^2 = 0.99$). Bland-Altman analysis (Fig. 4-5) showed no significant bias between the automated technique and the gold standard technique for ESV and EF. A small overestimation was found for EDV and mass. However, the bias expressed as error%/mean of the manual reference values resulted less than 8% for all the analyzed parameters. The 95% limits of agreement were relatively narrow (EDV=14ml, ESV=19ml, EF=10%, mass=15g), providing additional support to the good agreement between the two techniques (TABLE I).

Similarity metric results between manually traced and automatically obtained contours are shown in TABLE II. Inter-technique discordance in boundary position was estimated as

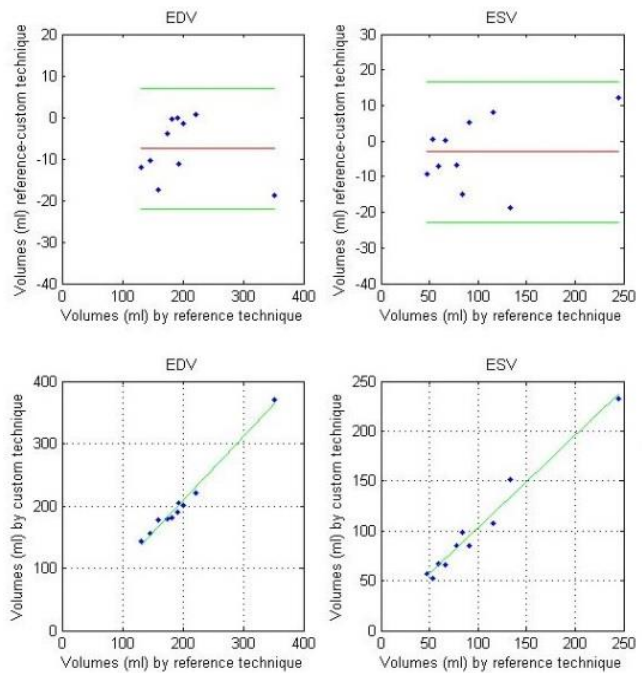


Figure 4. Bland-Altman (top) and linear regression (bottom) analyses of LV EDV and ESV obtained by the automated technique compared to the standard manual reference technique.

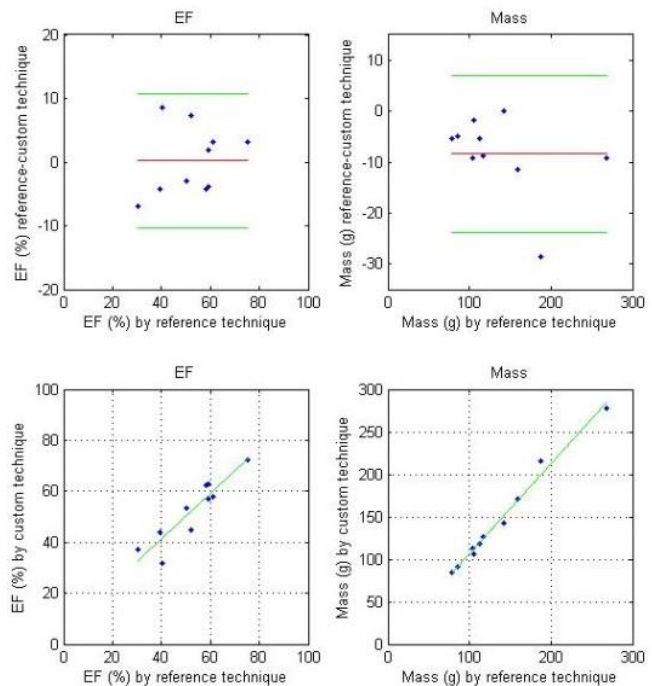


Figure 5. Bland-Altman (top) and linear regression (bottom) analyses of LV EF and mass obtained by the automated technique compared to the standard manual reference technique.

the point-by-point sum of absolute differences between the radial distances from the LV cavity area center normalized by the average contour radius. This discordance, was found to be more pronounced near the apex (Fig. 6).

TABLE II. RESULTS OF THE COMPARISON BETWEEN THE AUTOMATICALLY DETECTED AND MANUALLY TRACED ENDOCARDIAL AND EPICARDIAL CONTOURS IN ALL THE ANALYSED SLICES FOR THE ED AND ES FRAMES

Indices	ED		ES	
	Endocardium	Epicardium	Endocardium	Epicardium
Dice coefficient	0.93 ± 0.06	0.95 ± 0.03	0.91 ± 0.04	0.89 ± 0.11
Jaccard index	0.88 ± 0.09	0.90 ± 0.06	0.83 ± 0.07	0.82 ± 0.16
Hausdorff distance (pixel)	3.42 ± 0.46	3.72 ± 0.51	3.43 ± 0.51	3.84 ± 0.55
Hausdorff distance (mm)	1.71 ± 0.32	1.86 ± 0.39	1.72 ± 0.35	1.94 ± 0.42

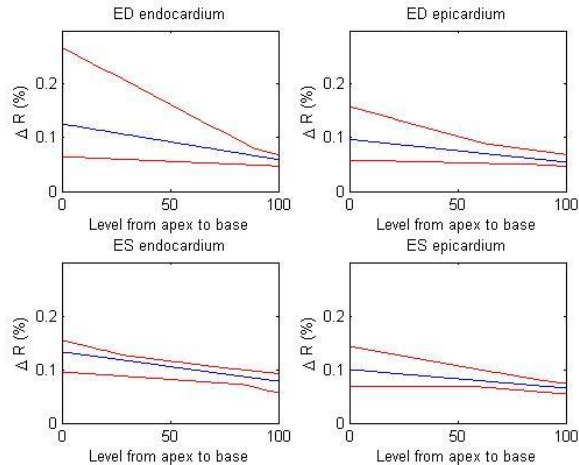


Figure 6. Distance between the two endo (left panels) and epicardial (right panels) boundaries (ΔR) at ED (top panels) and ES (bottom panels) at different levels of left ventricle from base to apex (every 1% of the LV length) averaged in 10 patients (blue lines represent mean values and red lines represent SD). Data shown percent of the measured values.

IV. DISCUSSION AND CONCLUSIONS

CMR imaging provides accurate measurements of LV volumes, EF and mass. Nevertheless, this procedure, based on manual tracing of endocardium and epicardium borders, is time-consuming and subjective. The proposed method overcomes these limitations. and agreements with conventional manual tracing were found.

The results obtained in this study have demonstrated the accuracy of the proposed technique, as indicated by minimal bias in Bland-Altman analysis and similarity indices. The increasing disparity near the LV apex is not surprising in view of the known relatively poor endocardial and epicardial definition in short axis slices as a result of partial volume artifacts that are more pronounced at this level of the ventricle.

The proposed technique allows the segmentation of all frames throughout the cardiac cycle and volume-time curves could be derived to assess information about diastolic and systolic function. In addition, the knowledge about the myocardium borders position could be the first step for a quantitative assessment of myocardial scar location and size from CMR. Preliminary results for scar segmentation, obtained applying a probabilistic level set method

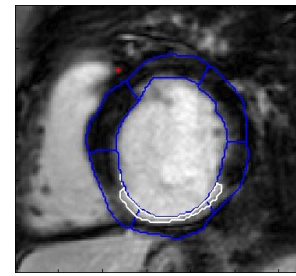


Figure 7. Scar delineation (white) using the probabilistic method and scar localization applying the six segments regional model of the myocardium (blue).

considering a noise Gaussian distribution for the gray level intensity of the scar, are shown in figure 7.

ACKNOWLEDGEMENT

We would like to thank Prof. Victor Mor-Avi and Prof. Amit Patel from the Department of Medicine at the University of Chicago for providing CMR datasets.

REFERENCES

- [1] D.J. Pennel, "Contemporary Review in Cardiovascular Medicine Cardiovascular Magnetic Resonance", *Circulation*, 2010, 121:692-705.
- [2] E. Angelie, P.J. De Koning, M.G. Danilouchkine, H.G. Van Assen, G. Koning, R.J. Van Der Geest, J.H. Reiber, "Optimizing the automatic segmentation of the left ventricle in magnetic resonance images", *Medical Physics*, 2005, 32(2):369-375.
- [3] C. Petitjean, J.-N. Dacher, "A review of segmentation methods in short axis cardiac MR images", *Medical Images Analysis*, 2011, 15:169-184.
- [4] Y.-L. Lu, K.A. Connelly, A.J. Dick, G.A. Wright, P.E. Radau, "Automatic functional analysis of left ventricle in cardiac cine MRI", *Quantitative Imaging in Medicine and Surgery*, 2013, 3(4):200-209.
- [5] C. Li, X. Jia, Y. Sun, "Improved semi-automated segmentation of cardiac CT and MR images", *2009 IEEE International Symposium on Biomedical Imaging: From Nano to Macro*, 2009, 25-28.
- [6] C. Corsi, F. Veronesi, C. Lamberti, D.M.E Bardo, E.B. Jamison, R. Lang, V. Mor-Avi, "Automated Frame-by-Frame Endocardial Border Detection for Quantitative Assessment of Left Ventricular Function: Validation and Clinical Feasibility", *Journal of Magnetic Resonance Imaging*, 2009, 29:560-568.
- [7] P. Perona, J. Malik, "Scale-Space and Edge Detection Using Anisotropic Diffusion", *IEEE Transactions on Pattern Analysis and Machine Intelligence*, 1990, 12(17):629-639.
- [8] R. Malladi, J.A. Sethian, B.C. Vemuri, "Shape modeling with front propagation: a level set approach", *IEEE Transactions on Pattern Analysis and Machine Intelligence*, 1995, 17(2):158-175.
- [9] R. El Berbari, I. Bloch, A. Redheuil, E. Angelini, E. Mousseaux, F. Frouin, A. Herment, "An automated myocardial segmentation in cardiac MRI", *Proceedings of the 29th Annual International Conference of the IEEE EMBS*, 2007, 4508-4511.